

NOTICE: this is the author's version of a work that was accepted for publication in *Geochimica et Cosmochimica Acta*. Changes resulting from the publishing process, such as peer review, editing, corrections, structural formatting, and other quality control mechanisms may not be reflected in this document. Changes may have been made to this work since it was submitted for publication. A definitive version was subsequently published in *GEOCHIMICA ET COSMOCHIMICA ACTA*, 75 (11), 2011, <http://dx.doi.org/10.1016/j.gca.2011.03.015>

Absence of seasonal patterns in MBT-CBT indices in mid-latitude soils

Johan W.H. Weijers^{1*}¶, Beth Bernhardt^{2*}, Francien Peterse^{3*}, Josef P. Werne^{2,4}, Jennifer A.J. Dungait⁵, Stefan Schouten³ and Jaap S. Sinninghe Damsté^{1,3}

¹Department of Earth Sciences – Geochemistry, Utrecht University, P.O. Box 80.021, 3508 TA Utrecht, The Netherlands;

²Large Lake Observatory and Department of Chemistry & Biochemistry, University of Minnesota Duluth, 10 University Dr., Duluth, MN, USA;

³Department of Marine Organic Biogeochemistry, Royal Netherlands Institute for Sea Research (NIOZ), P.O. Box 59, 1790 AB Den Burg-Texel, The Netherlands;

⁴work prepared while on leave at the Centre for Water Research, University of Western Australia, Crawley, Western Australia and WA-Organic and Isotope Geochemistry Centre, Curtin University of Technology, Bentley, Western Australia;

⁵Sustainable Soils and Grassland Systems Department, Rothamsted Research-North Wyke, Okehampton, Devon, EX20 2SB, United Kingdom.

* These authors contributed equally to this work

¶ Corresponding author: j.weijers@geo.uu.nl

1 **Abstract**

2 The degree of methylation and cyclisation of bacteria-derived branched glycerol dialkyl glycerol
3 tetraether (GDGT) membrane lipids in soils depends on temperature and soil pH. Expressed in
4 the Methylation index of Branched Tetraethers (MBT) and Cyclisation ratio of Branched
5 Tetraethers (CBT), these relationships are used to reconstruct past annual mean air temperature
6 (MAT) based on the distribution of branched GDGTs in ancient sediments; the MBT-CBT
7 proxy. Although it was shown that the best correlation of this proxy is with annual MAT, it
8 remains unknown whether a seasonal bias in temperature reconstructions could occur, such as
9 towards a seasonal period of ‘optimal growth’ of the, as yet, unidentified soil bacteria which
10 produce branched GDGTs. To investigate this possibility, soils were sampled from eight
11 different plots in the U.S.A. (Minnesota and Ohio), The Netherlands (Texel) and the U.K.
12 (Devon) in time series over one year and analyzed for their branched GDGT content. Further
13 analyses of the branched GDGTs present as core lipids (CLs; the presumed fossil pool) and
14 intact polar lipids (IPLs; the presumed extant pool) were undertaken for two of the investigated
15 soil plots. The amount of IPL-derived branched GDGTs is low relative to the branched GDGT
16 CLs, i.e. only 6-9% of the total branched GDGT pool. In all soils, no clear change was apparent
17 in the distribution of branched GDGT lipids (either core or IPL-derived) with seasonal
18 temperature change; the MBT-CBT temperature proxy gave similar temperature estimates year-
19 round, which generally matched the mean annual soil temperature. In addition to a lack of
20 coherent changes in relative distributions, concentrations of the branched GDGTs did not show
21 clear changes over the seasons. For IPL-derived GDGTs these results suggest that their turnover
22 time in soils is in the order of one year or more. Thus, our study does not provide evidence for
23 seasonal effects on the distribution of branched GDGTs in soils, at least at mid-latitudes, and
24 therefore no direct evidence for a bias of MBT-CBT reconstructed temperatures towards a
25 certain season of optimal growth of the source bacteria. If, however, there is a slight seasonal
26 preference of branched GDGT production, which can easily be obscured by natural variability
27 due to the heterogeneity of soils, then a seasonal bias may potentially still develop over time due
28 to the long turnover time of branched GDGTs.

29

1. INTRODUCTION

30
31
32
33
34
35
36
37
38
39
40
41
42
43
44
45
46
47
48
49
50
51
52
53
54

Branched glycerol dialkyl glycerol tetraethers (GDGTs) are core membrane lipids synthesised by as yet unknown bacteria (Weijers et al., 2006a). They occur in peat bogs and soils worldwide (Sinninghe Damsté et al., 2000; Leininger et al., 2006; Weijers et al., 2006b; Weijers et al., 2007c; Huguet et al., 2010a; Huguet et al., 2010b). Branched GDGTs consist of two alkyl chains ether bound to two glycerol units. The alkyl moieties contain two or three methyl groups each and in some, one of these methyl groups is incorporated into a cyclopentane moiety likely formed via internal cyclization (Weijers et al., 2006a). It has been shown previously that the relative distribution of the different branched GDGTs relates to soil pH and temperature (Weijers et al., 2007c; Peterse et al., 2009b; Peterse et al., 2010). The degree of cyclisation of the membrane lipids, expressed in the Cyclisation ratio of Branched Tetraethers (CBT) relates to soil pH, and the degree of methylation, expressed in the Methylation index of Branched Tetraethers (MBT) relates to both soil pH and temperature. These relationships are explained as adaptations by the GDGT-synthesizing microbe to ambient conditions in order to maintain the cell membrane in a liquid crystalline state, which is necessary to carry out essential cell membrane functions. In soils, the ambient temperature to which branched GDGT-producing bacteria adapt their cell membrane is most certainly soil temperature. As soil temperature data were not available in the global soil dataset studied by Weijers et al. (2007c), a correlation was made between branched GDGT distributions and annual mean air temperature (MAT), under the assumption that soil and air temperature are strongly related to each other and, on a yearly average basis, do not differ substantially from each other. Since these branched GDGTs are preserved in the sedimentary record, this relationship between MBT-CBT and annual MAT could be used as a proxy to reconstruct past temperatures (Weijers et al., 2007c).

55 After initial application in the Congo deep sea fan to reconstruct past MATs for tropical Africa since the last deglaciation (Weijers et al., 2007a), the MBT-CBT proxy is increasingly being used to reconstruct past MATs. These include, amongst others, deglacial Amazonia (Bendle et al., 2010) and East Asia (Peterse et al., 2011), the middle Pleistocene of southwestern North America (Fawcett et al., 2011), the Miocene of northwestern Europe (Donders et al., 2009), the Eocene-Oligocene boundary for East Greenland (Schouten et al., 2008), the early Eocene of the

61 Sierra Nevada (Hren et al., 2010) and the Palaeocene-Eocene Thermal Maximum (PETM) in the
62 Arctic (Weijers et al., 2007b). In some cases these palaeotemperature estimates are in agreement
63 with those of other proxies (e.g. Schouten et al., 2008; Ballantyne et al., 2010), however, a
64 potential bias to summer temperatures could not always be excluded. For example, reconstructed
65 MATs for the Arctic at the PETM are high (ca. 25°C, Weijers et al 2007b) and, although
66 comparable to sea surface temperature estimates, the authors suggested that due to three months
67 of darkness during polar winter these estimates might be biased towards summer temperature. A
68 comparison with much lower MAT estimates obtained from oxygen isotope ratios of biogenic
69 phosphate led Eberle et al. (2010) to suggest that MBT-CBT temperature estimates for the Arctic
70 during the PETM and early Eocene are indeed seasonally biased, i.e. towards the summer.
71 Nevertheless, a recent study by Puc at et al. (2010) pointed out that, because of methodological
72 biases, it could in fact be the MAT estimate based on these oxygen isotope ratios of biogenic
73 phosphate that might be underestimated by 4 to 8°C. In addition to these deep time applications,
74 Peterse et al. (2009a) showed for high latitude soils at Svalbard that MBT-CBT temperature
75 estimates were equal to measured annual MAT. However, Rueda et al. (2009) compared MBT-
76 CBT derived MAT estimates from a sediment record of the Skagerrak with instrumental
77 temperature data for the last 200 years and found that it best compared with summer
78 temperatures. Thus, there may be a seasonal bias in some MBT-CBT records, although Weijers
79 et al. (2007c) did not find better relationships between MBT-CBT and seasonal temperatures
80 than with annual mean temperatures.

81
82 Soil microbial communities are (indirectly) affected by changes in environmental conditions;
83 temperature being one of them (e.g. Frey et al., 2008 and references therein). In a recent study
84 where soils were incubated at elevated temperatures, Feng & Simpson (2009) observed that,
85 although the biomass and activity of soil microorganisms remained by and large constant, shifts
86 in the overall community composition of microorganisms (i.e., fungi vs. bacteria and gram-
87 negative vs. gram-positive bacteria) might occur as a result of temperature-induced substrate
88 constraints. Similar constraints occur for microbes when temperatures drop below optimum
89 conditions, resulting in limited microbial growth (Nedwell, 1999), and it is generally assumed
90 that microbial activity slows down and shifts to a maintenance-related metabolism when soil
91 freezes. Contrary to this view, however, Harrysson-Drotz et al. (2010) recently reported that both

92 catabolic and anabolic activities of heterotrophic microorganisms proceeded in frozen boreal
93 forest soil, including the biosynthesis of membrane lipids.

94
95 It is, therefore, not entirely clear whether the activity of branched-GDGT synthesizing bacteria in
96 soils is dependent on temperature. If this were to be the case, for example via temperature-
97 induced nutrient input to the soil which may vary according to the growing season of vegetation,
98 this could give rise to a preferential period of prosperity of branched-GDGT synthesizing
99 bacteria. Potentially, this might result in a seasonal bias in the temperature ‘recorded’ in the
100 membrane lipid composition in the soil. In order to investigate this hypothesis, we analyzed the
101 branched GDGT compositions in one year-long time series from eight different soil plots in
102 Minnesota and Ohio in the U.S.A., in Devon in the U.K. and on the island of Texel in The
103 Netherlands. The sites are all located at mid-latitudes where the seasonal contrasts in temperature
104 and growing season are pronounced. In addition to analyzing branched GDGTs as core lipids
105 (CL), i.e. without polar head groups and representing the fossil pool of GDGTs, we also
106 analyzed, in two soil plots, intact polar lipid (IPL)-derived branched GDGTs, i.e. those with a
107 polar head group and presumably derived from living cells. The results were compared with
108 temperature data from local weather stations as well as with *in situ* measured soil temperatures.

109 110 **2. MATERIALS AND METHODS**

111 112 **2.1. Soil Locations and Sampling**

113 114 *2.1.1. Itasca State Park and Bath Nature Preserve, United States of America*

115
116 Six soils were sampled in the United States, three in northwestern Minnesota near Elk Lake in
117 Itasca State Park, Clearwater County, and three in northeastern Ohio near Bath Pond, within
118 Bath Nature Preserve, Summit County. Northwestern Minnesota is characterized by a continental
119 climate with warm, humid summers and very cold winters (Peel et al., 2007). The annual MAT
120 in this part of the state is ca. 4°C and annual precipitation ca. 700 mm (KNMI, 1997). The
121 climate of northeastern Ohio is typical of humid continental regions with hot summers and cold
122 winters (Peel et al., 2007). The annual MAT in this area is ca. 10°C and annual precipitation ca.

123 900 mm (KNMI, 1997). At both sites, soils with three types of vegetation cover were sampled,
124 i.e. pine, deciduous and open field vegetation. The Itasca State Park soils were sampled from
125 September 2008 until August 2009, and the soils in Bath Nature Preserve from October 2008
126 until September 2009 by colleagues from the University of Akron. Duplicate soil cores were
127 collected at each sampling plot of 3x3 m using a hand auger or, in case of frozen soil, with
128 hammer and chisel. The 0-5 cm interval was used for analysis. All soil samples were stored
129 frozen at -20°C in ashed glass jars until further processing. Thermistors (NexSens micro-T
130 temperature loggers) were buried at a depth of ca. 15 cm in each of the soil plots in Minnesota
131 and Ohio (slightly deeper than the depth interval used for lipid analysis) to record soil
132 temperature 10 times a day (i.e, every 144 min). An additional thermistor was set ~1.5 m above
133 ground level to record ambient air temperatures at the sites. Thermistors recorded temperature
134 approximately every 2.5 h from September 2008 until October 2009.

135

136 2.1.2. Rowden Moor, United Kingdom

137

138 The time series from the U.K. was obtained from a grassland soil from the long-term
139 experimental research platform site at Rowden Moor near Okehampton (Devon, SW England).
140 Southwestern England is characterized by a humid maritime climate, which means that, in
141 contrast to the U.S.A. soils, seasonal extremes in temperature are smaller and that soil
142 temperature is above freezing point virtually all year round. The annual MAT at this site is 9.6°C
143 and the mean annual precipitation is 1056 mm (Harrod and Hogan, 2008). The soil has a silty
144 clay texture and remains very wet from autumn until early spring due to the virtually
145 impermeable clay layer at 30 cm depth (Harrod and Hogan, 2008). Samples were taken from the
146 control plot, a gently sloping undrained meadow that receives no fertilizer, although cows graze
147 the meadow for a defined period during the year. The vegetation consists of *Lolium perenne* with
148 patches of *Juncus effuses*. The soil was sampled at eighteen time points from November 2008
149 until November 2009. In order to minimize effects caused by the heterogeneous nature of a soil,
150 sampling was performed by taking five 30 cm long cores with a 3 cm diameter augur in an X-
151 shape over an area of approximately 30x30 m. The short cores were sliced in 10 cm depth
152 increments and stored at -20°C until sample processing. Upon freeze drying and removal of the
153 grass cover, the 0-10 cm interval increments were pooled and powdered using a ball mill and

154 subsequently extracted. Meteorological data (air temperature, precipitation and soil temperature
155 at 10 cm depth, all at hourly resolution) were obtained from the on-site official UK MET-Office
156 meteorological station.

157

158 2.1.3. *Texel, The Netherlands*

159

160 A sandy grassland soil was sampled near the Royal NIOZ on the island of Texel, which is in the
161 northwest of The Netherlands. The Netherlands is, like England, characterized by a maritime
162 climate with wet summers and mild winters. The annual MAT near Texel is 9.4°C and mean
163 annual precipitation is 750 mm (KNMI, 1997). The upper 10 cm of the soil was sampled
164 monthly from March 2008 until February 2009. Three samples were taken in a triangle shape on
165 a 1x1m plot and merged in order to minimize variability due to soil heterogeneity and stored
166 frozen at -20°C until further processing. Upon freeze-drying and grinding, the triplicate samples
167 were pooled. *In-situ* soil temperatures were measured at the time of sampling (always in the
168 morning) using an Ama-Digit ad 20th digital thermometer. Thus, in contrast with the soil plots
169 from the U.S.A. and the U.K., these soil temperatures do not represent daily averages. Average
170 monthly MATs were obtained from the nearest official weather station at De Kooy, which is
171 located on the mainland ca. 10 km from Texel (KNMI, 1997).

172

173 **2.2. Soil Extraction and Fractionation**

174

175 The soils from Elk Lake watershed and Bath Nature Preserve were processed at the Large Lakes
176 Observatory of the University of Minnesota, Duluth. Soils were freeze-dried and homogenized
177 with mortar and pestle after removal of root clumps and other large pieces of soil debris. Around
178 10 g of soil were solvent extracted using a DIONEX Accelerated Solvent Extractor (ASE) using
179 in *n*-hexane/dichloromethane (DCM) 9:1 (v/v) at 100 °C and 7.6×10^6 Pa to obtain a total lipid
180 extract (TLE). TLE aliquots were evaporated under nitrogen until dry, re-dissolved in *n*-
181 hexane/DCM 9:1 (v/v) and applied to an activated Al₂O₃ column. Apolar and polar fractions
182 were eluted with *n*-hexane/DCM 9:1 (v/v) and DCM/methanol (MeOH) 1:1 (v/v), respectively.

183

184 The Texel soil was processed at Royal NIOZ, and the Rowden Moor soil at both Rothamsted
185 Research-North Wyke (extraction) and Utrecht University (hydrolysis). For both soils, samples
186 were extracted using a modified Bligh & Dyer method in order to analyze both IPLs and CLs
187 (Bligh and Dyer, 1959). Freeze dried and powdered soil (ca. 10 g for the Rowden Moor soil and
188 ca. 3 g for the Texel soil) was ultrasonically extracted three times for 10 min. using a single-
189 phase solvent mixture of MeOH/DCM/phosphate buffer 10:5:4 (v/v/v). Upon centrifugation,
190 supernatants were collected and combined. DCM and phosphate buffer were added to the
191 combined extracts to create a new volume ratio of 5:5:4 (v/v/v) and obtain phase separation. The
192 extract (DCM phase) containing the GDGTs was separated from the residue (MeOH/phosphate
193 buffer phase) by centrifugation and collected. The residue phase was extracted twice more with
194 DCM and the combined extracts evaporated to near dryness using a rotary evaporator. The
195 extract was passed over a small column plugged with extracted cotton wool to remove any
196 remaining soil particles and then completely dried under a steady stream of pure N₂. The extract
197 was subsequently separated into a CL and IPL fraction over a small silica gel column according
198 to Pitcher et al. (Pitcher et al., 2009) with minor modifications. The CL fraction was obtained by
199 eluting with 5 column volumes of *n*-hexane:ethylacetate 1:1 (v/v) and the IPL fraction was
200 obtained by eluting with 5 column volumes of MeOH. A small aliquot of the obtained IPL
201 fraction was analyzed directly using high performance liquid chromatography/mass spectrometry
202 (HPLC/MS) to determine any carryover of CLs into the IPL fraction (see below). In order to
203 analyze IPLs as CLs, the IPL fraction was hydrolyzed to cleave off the polar head groups. To
204 this end the IPL fraction was refluxed for a minimum of 2h in 1.5N HCl in MeOH, cooled down
205 and neutralized to ~pH 5. To recover the sample, a small amount of double distilled or extracted
206 demineralized water was added and the mixture was extracted three times with DCM, which was
207 subsequently collected and evaporated to dryness. In addition to this acid hydrolysis, an aliquot
208 of the Rowden Moor soil IPL fraction was subjected to base hydrolysis in order to cleave off
209 phosphate bound head groups only. To this end the sample was refluxed for ca. 2h in a 1N KOH
210 in MeOH:H₂O 95:5 (v/v) mixture, cooled down, neutralized and recovered by extraction with
211 DCM similar as for the acid hydrolysis.

212
213 All branched GDGTs were quantified against a known amount of a C₄₆ GDGT standard (Huguet
214 et al., 2006) that was added to each fraction. Prior to analysis, the samples were ultrasonically

215 dissolved in a *n*-hexane:2-propanol 99:1 (v/v) solvent mixture in a concentration of ca 2 mg/ml
216 and filtered over an 0.45 µm PTFE filter (Alltech) to remove any particulates.

217

218 **2.3. GDGT Analysis**

219

220 All samples were analyzed at Royal NIOZ. GDGTs were analyzed using high performance liquid
221 chromatography – atmospheric pressure chemical ionization / mass spectrometry (HPLC-
222 APCI/MS) on an Agilent 1100 series LC/MSD SL according to Schouten et al. (2007) with
223 minor modifications. Briefly, separation was achieved on an analytical Alltech Prevail Cyano
224 column (150mm × 2.1mm, 3mm). Branched GDGTs were eluted with 90% A and 10% B, where
225 A = *n*-hexane and B = *n*-hexane:2-propanol 9:1 (v/v), isocratically for the first 5 min (flow rate
226 0.2 ml min⁻¹), thereafter with a linear gradient to 18% B in 45 min. Injection volume was 10 µl
227 for all samples. The different GDGTs were detected by scanning for their [M+H]⁺ ions
228 (protonated mass) in selected ion monitoring (SIM) mode and the peak area was used for
229 quantification. Absolute quantification was performed according to Huguet et al. (2006). MBT
230 indices and CBT ratios were calculated using peak areas and translated into annual MAT
231 estimates following the soil calibration described in Weijers et al. (2007c).

232 The standard error of estimate of the calibration formula is 5.5°C. The instrumental
233 reproducibility of the MAT estimate, based on several duplicate HPLC/MS analyses, was ±
234 0.3°C. The analytical error due to sample processing and analysis was determined by duplicate
235 processing of all Minnesota soil samples and by triplicate processing of four of the Rowden
236 Moor soil samples. For the Minnesota soils, the average standard deviation of the MAT estimates
237 was 1.1°C and for the Rowden Moor soil the average standard deviation was 0.4°C for the CLs
238 and 1.0°C for the IPLs. For the concentration of GDGTs, the analytical error was ca. 25% for the
239 Minnesota soils and ca. 10% for the Rowden Moor soil.

240

241 **2.4. Correction for Carryover of Core Lipids**

242

243 As concentrations of IPL-derived branched GDGTs are substantially lower than those of the CL
244 fractions and separation of both fractions over a silica-gel column does not always results in a
245 full separation (likely depending on the extract composition, see Pitcher et al., 2009), small

246 aliquots of the IPL fraction were analyzed using HPLC/MS without further hydrolysis to screen
247 for the presence of branched GDGT CLs. It appeared that the carryover of CLs into the IPL
248 fraction is minor, i.e. ca. 2% of all CLs ended up in the IPL fraction, both for Rowden Moor soil
249 and for the Texel soil. However, given the much lower concentrations of GDGTs in the IPL
250 fraction relative to the CL fraction, this pool of leaked CLs accounted for ca. 23% of all GDGTs
251 measured in the hydrolyzed fraction in Rowden Moor soil and ca. 30% for the Texel soil.
252 Therefore, the reported concentrations of IPL-derived branched GDGTs were corrected for this.
253 As this (small) fraction of leaked branched GDGT CLs might have a distribution (and thus
254 ‘temperature signature’) that could deviate from the IPL-derived GDGTs, a correction has also
255 been made for the reconstructed MAT based on the IPL-derived GDGTs. This correction was
256 made by subtracting concentrations of individual branched GDGTs of the leaked CL fraction
257 from the concentrations of branched GDGTs in the IPL-derived fraction, and recalculating MAT
258 based on the new distribution. The resulting correction was minimal in the Rowden Moor soil,
259 i.e. 0.4°C on average. For the Texel soil this correction is slightly larger, i.e. 1.4°C on average.

260

261

3. RESULTS AND DISCUSSION

262

3.1. Instrumental Temperature Data

263

264
265 All four sites showed clear differences in seasonal air temperature. Due to the maritime climate
266 of western Europe, however, the maximum difference in monthly mean air temperatures at Texel
267 and Rowden Moor, i.e. 16 and 14°C, respectively, was lower than at the sites in Itasca State Park
268 (Minnesota) and Bath Nature Preserve (Ohio), i.e. 33 and 26°C, that experience a continental
269 climate (Fig. 1). Daily soil temperatures as measured in the Minnesota, Ohio and Rowden Moor
270 soils showed lower extremes than the measured air temperature due to the heat capacity of soils.
271 Among the Minnesota soils, the pine plot showed slightly lower amplitudes in soil temperature
272 than the open field plot and a delayed response to warming in spring, both most likely as a result
273 of the insulating effect of the vegetation cover. This effect was less pronounced for the Ohio
274 soils. Unfortunately, the thermistor from the deciduous plot in Ohio could not be recovered and
275 the one from the deciduous plot in Minnesota malfunctioned, so we did not obtain *in situ*
276 temperature data for these soils. Under the assumption that the temperature in the deciduous

277 forest soil will not deviate substantially from the temperature in the pine forest soil, the latter was
278 used for comparison with the MBT-CBT derived MATs in the deciduous forest soil. For all soils
279 for which *in-situ* soil temperature data were available, the annual mean soil temperature was
280 higher than the annual MAT (Fig. 1). In the Minnesota and Ohio soils this was mainly due to the
281 fact that winter soil temperatures never reach far below freezing point. For Rowden Moor soil
282 this is principally due to soil temperatures in summer that are about 2°C higher than air
283 temperatures, probably due to the insulating effect of the grass cover at night. This difference
284 between mean air and mean soil temperature was smallest in the pine forest soil in Ohio (0.4°C)
285 and largest in the open field soil from Minnesota (4.4°C). The difference for the open field
286 grassland at Rowden Moor was 1.3°C.

287

288 **3.2. Branched GDGT Core Lipids**

289

290 Concentrations of branched GDGT CLs were determined for all soils and fall within ranges
291 reported in other studies (Kim et al., 2006; Weijers et al., 2006b; Peterse et al., 2009b; Huguet et
292 al., 2010b). For the Minnesota soils, annual averaged concentrations were 240 ± 60 (standard
293 deviation) ng g^{-1} dry weight soil (dws) for the open field, $290 \pm 70 \text{ ng g}^{-1}$ dws for the pine forest
294 and $430 \pm 110 \text{ ng g}^{-1}$ dws for the deciduous forest time series, respectively (Fig. 2a). For the
295 Ohio soils the annual averaged concentrations were $170 \pm 70 \text{ ng g}^{-1}$ dws for the open field, 2500
296 $\pm 1250 \text{ ng g}^{-1}$ dws for the pine forest and $310 \pm 170 \text{ ng g}^{-1}$ dws for the deciduous forest (Fig. 2b).
297 Annual averaged branched GDGT CL concentrations for the Texel and the Rowden Moor
298 grassland soils were $600 \pm 120 \text{ ng g}^{-1}$ dws (Fig. 2c) and $1600 \pm 300 \text{ ng g}^{-1}$ dws (Fig. 2d),
299 respectively. In the Minnesota open field soil, the Ohio soils, the Texel soil and the Rowden
300 Moor soil no seasonal trend in branched GDGT CL concentrations was apparent (Fig. 2). For the
301 Minnesota pine forest and deciduous forest soils somewhat higher concentrations seem to be
302 present in July and August. For the Rowden Moor soil, precipitation data were available, but no
303 relation with precipitation was found.

304

305 MBT-CBT reconstructed temperatures (based on the CLs) remained constant throughout the year
306 in all soils, with variations in MAT estimates within the same soil usually $< 5^\circ\text{C}$ in the
307 Minnesota and Ohio pine forest soils (Figs. 3, 4), $< 3^\circ\text{C}$ in the deciduous forest and open field

308 soils from the same sites (Figs. 3, 4), $<2^{\circ}\text{C}$ in the Texel soil (Fig. 5) and $<1^{\circ}\text{C}$ in the Rowden
309 Moor soil (Fig. 6). The observed variations did not coincide with seasonal variations in soil
310 temperature. The average MBT-CBT derived temperatures for the Minnesota soils were 10.3°C
311 $\pm 1.2^{\circ}\text{C}$ (standard deviation) for the open field site and $9.9^{\circ}\text{C} \pm 1.9^{\circ}\text{C}$ for the pine site, which are
312 clearly warmer than the annual MAT of 3.8°C but closer to the annual mean soil temperature of
313 8.2°C at the open field site and 6.0°C at the pine site (Fig. 1). For the Ohio soils, the average
314 MBT-CBT derived temperatures were $8.4^{\circ}\text{C} \pm 0.9^{\circ}\text{C}$ for the open field and $12.6^{\circ}\text{C} \pm 1.6^{\circ}\text{C}$ for
315 the pine plot, which are both close to the annual MAT of 9.9°C and the measured annual mean
316 soil temperature of 10.4°C at the open field site and 10.0°C at the pine site (Fig. 1). Strikingly,
317 MBT-CBT reconstructed temperatures for the deciduous soils in both Minnesota and Ohio were
318 high, i.e. $14.0^{\circ}\text{C} \pm 0.9^{\circ}\text{C}$ and $19.2^{\circ}\text{C} \pm 1.0^{\circ}\text{C}$, respectively (Figs. 3, 4). This is 10.2 and 9.6°C ,
319 respectively, higher than measured annual MAT and 8.0 and 9.2°C , respectively, higher than
320 annual mean soil temperature under pine forest (Fig. 1). Unfortunately, no soil temperature data
321 were available for both deciduous plots, but it seems unlikely that these would be that much
322 higher than under pine forest. This makes these soils the only two in this set of eight to give
323 reconstructed MATs that show offsets to measured temperature larger than the standard error of
324 estimate of the soil calibration dataset of ca. 5.5°C (Weijers et al., 2007b). The reason for this
325 deviating pattern is, at present, not clear. For the Texel soil, the MBT-CBT reconstructed
326 temperature based on the CLs was $7.1^{\circ}\text{C} \pm 0.8^{\circ}\text{C}$, which is slightly lower than the annual MAT
327 for this area of 9.4°C (Fig. 1, 5). Of the eight soils sampled, the reconstructed temperature based
328 on CLs in the Rowden Moor soil was the most stable throughout the year at $11.1^{\circ}\text{C} \pm 0.7^{\circ}\text{C}$,
329 which is close to annual MAT of 9.6°C and equal to the annual mean soil temperature of 11.1°C
330 (Fig. 2, 6). One exception is the sample from May 15th that gave a reconstructed temperature of
331 9°C . This is clearly lower than the reconstructed temperature for the sample taken a week earlier
332 (May 7th; 11.2°C) and that of June 4th (11.6°C). This particular sample is also an outlier in terms
333 of the concentration of branched GDGTs.

334

335 In all soils for which continuous soil temperature data are available, i.e. Minnesota open field
336 and pine forest, Ohio open field and pine forest and Rowden Moor soil, the MBT-CBT
337 reconstructed temperature was closer to the measured annual mean soil temperature than to the
338 measured annual MAT. This is surprising as in the soil calibration dataset a calibration was made

339 with annual MAT and not with soil temperature (Weijers et al., 2007c). As is also evident from
340 the temperature data shown here, soil and air temperature are not identical, and more
341 importantly, the offset differs with region and type of vegetation. The observed variation
342 depends on a range of factors, including differences in vegetation cover, water content (which
343 determines heat capacity) and latitude (intensity of winter frost conditions) of the soil (e.g. Oliver
344 et al., 1987). The fact that MBT-CBT reconstructed temperatures do not always exactly reflect
345 annual MAT implies that, as suggested by Weijers et al. (2007c), a substantial part of the scatter
346 present in the MBT-CBT calibration may result from this variation in the offset between soil and
347 air temperatures.

348

349 The branched GDGT CL assemblages in the eight soils analyzed, clearly showed no response to
350 seasonal changes in temperature. This lack of any seasonal trend may be ascribed to a standing
351 stock of CLs whose abundance is much larger than new production of branched GDGTs over a
352 seasonal cycle. Earlier work, comparing the amount of branched GDGT CLs in a peat core with
353 cell numbers of the most dominant bacteria, suggested the presence of such a standing stock of
354 CLs (Weijers et al., 2009). Indeed, Weijers et al. (2010) showed by means of the stable carbon
355 isotopic composition of the branched alkanes released from branched GDGTs that their turnover
356 time, at least in mid-latitude cropland soils, is near 20 years, and Peterse et al. (2010) showed
357 that the branched GDGT (CLs) composition in a grassland soil had fully adjusted to a
358 manipulated change in pH after 40 years. These studies indicate that the standing stock of
359 branched GDGT CLs turns over on timescales of decades and that, consequently, the distribution
360 of branched GDGT CLs in a given soil is adjusted to new environmental conditions at these time
361 scales. This turnover time of decades for branched GDGT CLs also implies that the variation in
362 CL concentration as found in some soils has to be interpreted with care. It seems unlikely that the
363 pool of CLs is suddenly halved or doubled in a month. These variations are likely to be, at least
364 partly, the result of the well-known spatial heterogeneity of soils. From the work presented here,
365 it is clear that the branched GDGT CL distribution does not adjust to changes in ambient
366 conditions (at least temperature) on time scales <1 year. The turnover time of near 20 years
367 implies that the MAT signal documented by the branched GDGT CLs is a time-integrated signal
368 over previous years (with the potential for a greater weighting for more recent years, though this

369 remains to be demonstrated).

370

371 **3.3. Branched GDGT Intact Polar Lipids**

372

373 *3.3.1. Acid-hydrolyzed IPLs*

374

375 Since branched GDGT CL distributions did not show a response to seasonal variations, we
376 analyzed IPL-derived branched GDGTs which are presumably a better reflection of the extant
377 soil bacterial population. Therefore, for the Texel soil and Rowden Moor soil, IPL branched
378 GDGTs were separated from the CLs, hydrolyzed and analyzed as CLs. Concentrations of these
379 IPL-derived branched GDGTs varied from ca. $40 \pm 15 \text{ ng g}^{-1} \text{ dws}$ in the Texel soil (Fig. 2c) to
380 ca. $150 \pm 30 \text{ ng g}^{-1} \text{ dws}$ in the Rowden Moor soil (Fig. 2d). However, as observed for the CLs,
381 no relationship was apparent between the concentration of the IPL-derived branched GDGTs and
382 temperature (Figs. 2, 5, 6). The IPL fraction of the branched GDGTs in the soils only accounted
383 for 6% (Texel soil) and 9% (Rowden Moor soil) of the total branched GDGT pool, which is only
384 slightly higher than the value of 4% reported by Liu et al. (2010) in a German peat bog.
385 Assuming that all IPLs are derived from extant biomass, this indicates that more than 90% of the
386 branched GDGTs present in the soil are in a fossil (CL) form.

387

388 Although temperature estimates reconstructed using branched GDGTs from the IPL fraction
389 were expected to better reflect seasonal temperature, this is not the case. In the Texel soil,
390 temperature reconstructions based on the IPL-derived branched GDGTs showed values that are
391 similar to the estimates based on the CL fraction (Fig. 5; average $6.7^\circ\text{C} \pm 1.0^\circ\text{C}$). Except for
392 April and July, the difference between the estimated temperatures from both fractions was $<1^\circ\text{C}$,
393 i.e. within analytical error. In the Rowden Moor soil, temperature estimates based on GDGTs
394 from the IPL (acid-hydrolyzed) fraction differed slightly more from the estimates based on the
395 CL fraction (Fig. 6; average $10.6^\circ\text{C} \pm 2.2^\circ\text{C}$). IPL based temperature estimates were either up to
396 2.4°C higher (September) or down to 3.4°C lower (February) than the CL based estimates of the
397 same months. Although these two extremes might suggest some kind of adaptation, it has to be
398 noted that higher IPL-based than CL-based temperature estimates also occurred in winter and
399 lower estimates in summer. A Student's t-test shows that IPL-derived MAT estimates for the

400 warm part of the year (in this case defined as May – October) were not significantly higher than
401 CL-derived MAT estimates, and that IPL-derived MAT estimates for the cool part of the year
402 (November – April) were only just significantly lower than CL-derived MAT estimates, in both
403 cases at a 95% confidence interval. This indicates that the data indeed are scattered and that there
404 is no unambiguous clear trend in IPL-derived MAT related to seasonal changes in temperature
405 (Fig. 6).

406
407 These results suggest that, as with the CL branched GDGTs, the turnover of IPL-derived
408 branched GDGTs in soil is rather slow, albeit perhaps faster than for CL branched GDGTs. One
409 potential cause for this would be if IPLs are also preserved over time scales of months to years,
410 as this would result in a smoothing of the seasonal temperature signal. Harvey et al. (1986)
411 observed that bacterial phospholipids degrade relatively fast, whereas glycosidically bound ether
412 lipids degrade much more slowly. Based on modeling of degradation rates in the marine
413 environment, Schouten et al. (2010) recently proposed that a significant portion of glycosidic
414 GDGTs could indeed be preserved in the sedimentary record. Liu et al. (2010) recently reported
415 the occurrence of branched GDGT IPLs containing glycosidic head groups in a German peat
416 bog, but no IPLs containing a phospho head group, suggesting that glycosidic branched GDGT
417 IPLs may indeed be preserved over time scales longer than those of phospho IPLs.

418

419 *3.3.2. Base-hydrolyzed IPLs*

420

421 To investigate whether the majority of the branched GDGT IPL pool consisted of glycolipids, an
422 aliquot of the IPL fraction of the Rowden Moor soil samples was subjected to base hydrolysis,
423 which only cleaves ester bound phospho head groups and not ether bound glycosidic head
424 groups. The average concentration of the phospho IPL-derived branched GDGTs was ca. $110 \pm$
425 $30 \text{ ng g}^{-1} \text{ dws}$ (Fig. 2d). Comparison with the yield of the acid-hydrolyzed IPL aliquot, which
426 was ca. $150 \text{ ng g}^{-1} \text{ dws}$ and represents the sum of phospho IPLs and glycosidic IPLs, suggests
427 that the majority of the branched GDGT IPLs contain ester bound phosphate head groups. Given
428 that glycosidic branched GDGTs might even be enriched in abundance over time relative to the
429 phospho IPLs due to their supposedly slower degradation rate, this suggests that the amount of
430 glycolipids produced by the branched-GDGT synthesizing bacteria is small relative to the

431 phospholipids. This is in apparent contradiction with the work of Liu et al. (2010) who only
432 found glycosidic head groups for the branched GDGTs, although it needs to be stressed that this
433 was in a peat bog rather than a soil.

434
435 If the branched GDGTs released upon base hydrolysis are derived from (more labile)
436 phospholipid branched GDGTs, then they may be a better reflection of the living bacterial
437 population. However, also in the base-hydrolyzed fraction, GDGT concentrations showed no
438 relationship with temperature over the seasons (Fig. 6). The MBT-CBT reconstructed MAT
439 based on the base-hydrolyzed IPL fraction (average $10.7^{\circ}\text{C} \pm 2.1^{\circ}\text{C}$) also showed no noticeable
440 difference with temperatures reconstructed for the acid-hydrolyzed fraction or the CL fraction
441 (Fig. 6). Except for June (-1.2°C), the differences between reconstructed MATs in the acid- and
442 base-hydrolyzed samples were within 1°C , and thus within analytical uncertainty. In fact, this
443 similarity is not strange given that the majority of IPLs seems to consist of phospho bound IPLs,
444 which are measured in both the acid- and the base-hydrolyzed fraction. Thus, the small
445 differences in estimated MAT over the course of a year, based on the acid-hydrolysed IPL
446 fractions both in the Texel soil and in the Rowden Moor soil, is likely not due to the specific
447 presence of larger amounts of preserved glycosidic IPLs.

448
449 Assuming then that IPL-derived branched GDGTs represent living biomass, it might be that
450 branched-GDGT synthesizing bacteria have low cell division rates and exhibit relatively long
451 regeneration times. This would have a similar smoothing effect as with fossil GDGTs in the CL
452 fraction, since part of the IPLs detected at a given point in time could be produced several
453 months earlier. Indeed, many bacteria are known to grow slowly. An extreme example are the
454 anammox bacteria with cell division times up to a month (Van de Graaf et al., 1996; Strous et al.,
455 1998). Also several Acidobacteria, the bacterial phylum potentially containing the branched-
456 GDGT synthesizing bacteria (Weijers et al., 2009), are relatively slow growers (Eichorst et al.,
457 2007; Davis et al., 2011). Given that there is no systematic variation over the year in the MBT-
458 CBT reconstructed temperatures for the IPL-derived branched GDGTs, the combined effects of
459 suspected slow regeneration times of the responsible bacteria and the slow degradation rate of
460 IPLs suggest a perceived turnover time of IPLs in these soils in the order of a year.

461

4. IMPLICATIONS

462
463
464
465
466
467
468
469
470
471
472
473
474
475
476
477
478
479
480
481
482

Previous studies have shown that branched GDGT-synthesizing soil microbes adapt their membrane lipid distributions to pH and temperature (Weijers et al., 2007c; Peterse et al., 2009b; Peterse et al., 2010). These are the ambient pH and temperature and thus soil pH and soil temperature. Since for the global soil calibration dataset no soil temperature data were available, a calibration was made with annual MAT under the assumption that the two are roughly equal. Although on larger regional and global scales this will be true, on a local scale, as is evident from our study, soil and air temperature are not equal, and more importantly, also the offset between the two is not the same everywhere. It is important to realize, therefore, that, as also indicated by Weijers et al. (2007c), a large part of the scatter in the MBT-CBT calibration with annual MAT (which gives a standard error of estimate of ca. 5°C) may result from this offset between soil and air temperature. As a consequence, absolute temperatures reconstructed with the MBT-CBT proxy, though calibrated with annual MAT, do not always exactly reflect annual MAT, like in some of the soils studied here. On the larger scale, nevertheless, the MBT-CBT proxy is still thought to be able to provide reasonable estimates of past annual MAT and, especially, of changes therein (e.g. Weijers et al., 2007a). It is the reconstructed absolute temperature that is associated with a slightly larger error (ca. 5°C). This could only be better constrained when pure cultures of the branched-GDGT synthesizing bacteria are available or when studies like the current one, where soil temperatures are monitored over the annual cycle, are performed on a wide variety of soils.

483
484
485
486
487
488
489
490
491
492

Our study clearly shows that in mid-latitude soils, no seasonal trends are apparent in the concentration and distribution of branched GDGT CLs. Also in IPL-derived branched GDGT concentration and distribution no clear seasonal trends are apparent. Thus, from the data presented here, it seems that palaeoclimate reconstructions based on branched GDGT CL distributions do not suffer from particular seasonal biases. However, we cannot fully exclude the hypothesis that production of GDGTs in a certain season could be slightly higher than in others, but that these monthly differences are obscured as they are very small relative to the standing stock of GDGTs. A turnover time of 20 years for CLs implies that ca. 5% of the pool is refreshed in a given year, or ca. 0.4% per month. Monthly variations in this small percentage will not be

493 detectable. Similarly, for the IPL-derived GDGT pool small variations in its turnover rate of ca.
494 8% per month (based on an assumed turnover time in the order of a year), will likely be obscured
495 by variability due to the heterogeneity of soils. Over the course of 20 years, these small seasonal
496 biases might influence the long term average distribution of branched GDGT CLs and thus the
497 temperature reconstructed using the MBT-CBT proxy. This effect might be expected to be
498 stronger in soils experiencing stronger contrasts between seasons. If such an offset exists, it is,
499 however, not necessarily directed towards a particular season, given that the Texel soil, or the
500 Ohio open field soil, for example, gave reconstructed temperatures lower than annual MAT
501 while the Minnesota soils give reconstructed temperature higher than annual MAT.

502

503 The results presented here are derived from soils from mid-latitudes. In the tropics, seasonal
504 contrasts in temperature are much smaller and seasonal biases in MBT-CBT reconstructed MATs
505 are, therefore, expected to be much less of an issue in these climates. Our study, however, cannot
506 completely rule out the presence of a seasonal bias at high latitude sites like the Arctic, as a
507 period of up to three months of darkness may have, indirectly via vegetation and nutrient flows,
508 substantial effects on the soil microbial communities. For present-day Svalbard, nevertheless,
509 reconstructed MAT based on branched GDGT CL distributions is close to measured annual
510 MAT (i.e. -4°C and -6°C , respectively, Peterse et al., 2009a).

511

512 The fact that branched GDGT CLs represent a standing stock that has accumulated over the
513 course of years (ca. 20 years, Weijers et al., 2010) not only explains why the MBT-CBT proxy in
514 soils relates with an annual average temperature, it also implies that the proxy can only be
515 applied on geological time scales with resolutions larger than several decades. Most applications
516 that used the MBT-CBT proxy in obtaining records of MAT estimates have been obtained from
517 sites receiving fluvial transported sediments and are, therefore, already considerably temporally
518 smoothed (e.g. Weijers et al., 2007a), but this issue could be important in cases where the proxy
519 is used in high resolution studies of peat or loess deposits.

520

521

522

523 *Acknowledgements.* Dr. L. Schwark and two anonymous reviewers are acknowledged for
524 providing helpful comments that have improved the earlier version of our manuscript. This study
525 was made possible by financial support from the Netherlands Organisation for Scientific
526 Research (NWO) through a VENI grant to J.W.H.W.. The European Science Foundation is
527 thanked for providing an ESF-MOLTER Short Visit Grant to J.W.H.W. that enabled a stay at
528 Rothamsted Research – North Wyke. F.P., S.S. and J.S.D. thank the Darwin Center for
529 Biogeosciences and the Royal NIOZ for funding. S.S. and J.S.D. received funding from the ERC
530 project PACEMAKER. J.P.W. received funding from the US National Science Foundation grant
531 EAR-0745658 and acknowledges support from the Gladden Fellowship. This work forms
532 contribution 2400-JW at the Centre for Water Research, The University of Western Australia.
533 Matt Kemp and Lisa Park from the University of Akron are gratefully acknowledged for
534 sampling assistance.

535

536

537

538

Reference List

539

- 540 Ballantyne A. P., Greenwood D. R., Sinninghe Damsté J. S., Csank A. Z., Eberle J. J., and
541 Rybczynski N. (2010) Significantly warmer Arctic surface temperatures during the Pliocene
542 indicated by multiple independent proxies. *Geology* **38**, 603-606.
- 543 Bendle J. A., Weijers J. W. H., Maslin M. A., Sinninghe Damsté J. S., Schouten S., Hopmans E.
544 C., Boot C. S., and Pancost R. D. (2010) Major changes in glacial and Holocene terrestrial
545 temperatures and sources of organic carbon recorded in the Amazon fan by tetraether lipids.
546 *Geochem. Geophys. Geosyst.* **11**, 1-13, Q12007, doi:10.1029/2010GC003308.
- 547 Bligh E. G. and Dyer W. J. (1959) A rapid method of total lipid extraction and purification. *Can.*
548 *J. Biochem. Physiol.* **37**, 911-917.
- 549 Davis K. E. R., Sangwan P., and Janssen P. H. (2011) *Acidobacteria*, *Rubrobacteridae* and
550 *Chloroflexi* are abundant among very slow-growing and mini-colony-forming soil bacteria.
551 *Environ. Microbiol.* in press, doi:10.1111/j.1462-2920.2010.02384.x.
- 552 Donders T. H., Weijers J. W. H., Munsterman D. K., Hoeve M. L. K. V., Buckles L. K., Pancost
553 R. D., Schouten S., Sinninghe Damsté J. S., and Brinkhuis H. (2009) Strong climate coupling
554 of terrestrial and marine environments in the Miocene of northwest Europe. *Earth Planet. Sci.*
555 *Lett.* **281**, 215-225.

- 556 Drotz S. H., Sparrman T., Nilsson M. B., Schleucher J., and Oquist M. G. (2010) Both catabolic
557 and anabolic heterotrophic microbial activity proceed in frozen soils. *Proc. Natl. Acad. Sci.*
558 *USA* **107**, 21046-21051.
- 559 Eberle J. J., Fricke H. C., Humphrey J. D., Hackett L., Newbrey M. G., and Hutchison J. H.
560 (2010) Seasonal variability in Arctic temperatures during early Eocene time. *Earth Planet.*
561 *Sci. Lett.* **296**, 481-486.
- 562 Eichorst S. A., Breznak J. A., and Schmidt T. M. (2007) Isolation and characterization of soil
563 bacteria that define *Teniglobus* gen. nov., in the phylum Acidobacteria. *Appl. Environ.*
564 *Microbiol.* **73**, 2708-2717.
- 565 Fawcett P., Werne J.P., Anderson R., Heikoop J., Brown E., Berke M., Smith S., Goff F., Hurley
566 L., Cisneros-Dozal M., Schouten S., Sinninghe Damsté J.S., Huang Y., Toney J., Fessenden
567 J., WoldeGabriel G., Atudorei V., Geissman J., Allen C. (2011) Extended megadroughts in
568 the southwestern United States during Pleistocene interglacials. *Nature. In press.*
569 DOI:10.1038/nature09839.
- 570 Feng X. J. and Simpson M. J. (2009) Temperature and substrate controls on microbial
571 phospholipid fatty acid composition during incubation of grassland soils contrasting in
572 organic matter quality. *Soil Biol. Biochem.* **41**, 804-812.
- 573 Frey S. D., Drijber R., Smith H., and Melillo J. (2008) Microbial biomass, functional capacity,
574 and community structure after 12 years of soil warming. *Soil Biol. Biochem.* **40**, 2904-2907.
- 575 Harrod T. R. and Hogan D. V. (2008) The soils of North Wyke and Rowden. Online available at
576 [http://www.northwyke.bbsrc.ac.uk/assets/pdf_files/Soils%20of%20NW%20%20Rowden%20](http://www.northwyke.bbsrc.ac.uk/assets/pdf_files/Soils%20of%20NW%20%20Rowden%202.pdf)
577 [2.pdf](http://www.northwyke.bbsrc.ac.uk/assets/pdf_files/Soils%20of%20NW%20%20Rowden%202.pdf).
- 578 Harvey H. R., Fallon R. D., and Patton J. S. (1986) The effect of organic matter and oxygen on
579 the degradation of bacterial membrane lipids in marine sediments. *Geochim. Cosmochim.*
580 *Acta* **50**, 795-804.
- 581 Hren M. T., Pagani M., Erwin D.M., and Brandon M. (2010) Biomarker reconstruction of the
582 early Eocene paleotopography and paleoclimate of the northern Sierra Nevada. *Geology* **38**, 7-
583 10.
- 584 Huguet A., Fosse C., Laggoun-Defarge F., Toussaint M. L., and Derenne S. (2010a) Occurrence
585 and distribution of glycerol dialkyl glycerol tetraethers in a French peat bog. *Org. Geochem.*
586 **41**, 559-572.
- 587 Huguet A., Fosse C., Metzger P., Fritsch E., and Derenne S. (2010b) Occurrence and distribution
588 of extractable glycerol dialkyl glycerol tetraethers in podzols. *Org. Geochem.* **41**, 291-301.
- 589 Huguet C., Hopmans E. C., Febo-Ayala W., Thompson D. H., Sinninghe Damsté J. S., and
590 Schouten S. (2006) An improved method to determine the absolute abundance of glycerol
591 dibiphytanyl glycerol tetraether lipids. *Org. Geochem.* **37**, 1036-1041.

- 592 Kim J.-H., Schouten S., Buscail R., Ludwig W., Bonnin J., Sinninghe Damsté J. S., and Bourrin
593 F. (2006) Origin and distribution of terrestrial organic matter in the NW Mediterranean (Gulf
594 of Lion): application of the newly developed BIT index. *Geochem. Geophys. Geosyst.* **7**,
595 Q11017, doi:10.1029/2006GC001306.
- 596 KNMI (1997) World Climate Information (WKI) 2.0. Online available at:
597 <http://www.knmi.nl/klimatologie/normalen1971-2000/wki.html>, Koninklijk Nederlands
598 Meteorologisch Instituut (KNMI), De Bilt, The Netherlands.
- 599 Leininger S., Urich T., Schloter M., Schwark L., Qi J., Nicol G. W., Prosser J. I., Schuster S. C.,
600 and Schleper C. (2006) Archaea predominate among ammonia-oxidizing prokaryotes in soils.
601 *Nature* **442**, 806-809.
- 602 Liu X.-L., Leider A., Gillespie A., Gröger J., Versteegh G. J. M., and Hinrichs K.-U. (2010)
603 Identification of polar lipid precursors of the ubiquitous branched GDGT orphan lipids in a
604 peat bog in Northern Germany. *Org. Geochem.* **41**, 653-660.
- 605 Nedwell D. B. (1999) Effect of low temperature on microbial growth: lowered affinity for
606 substrates limits growth at low temperature. *FEMS Microbiol. Ecol.* **30**, 101-111.
- 607 Oliver S. A., Oliver H. R., Wallace J. S., and Roberts A. M. (1987) Soil heat-flux and
608 temperature-variation with vegetation, soil type and climate. *Agricult. Forest Meteorol.* **39**,
609 257-269.
- 610 Peel M. C., Finlayson B. L., and McMahon T. A. (2007) Updated world map of the Köppen-
611 Geiger climate classification. *Hydrol. Earth Syst. Sci.* **11**, 1633-1644.
- 612 Peterse F., Kim J.-H., Schouten S., Klitgaard Kristensen D., Koç N., and Sinninghe Damsté J. S.
613 (2009a) Constraints on the application of the MBT/CBT palaeothermometer at high latitude
614 environments (Svalbard, Norway). *Org. Geochem.* **40**, 692-699.
- 615 Peterse F., Nicol G. W., Schouten S., and Sinninghe Damsté J. S. (2010) Influence of soil pH on
616 the abundance and distribution of core and intact polar lipid-derived branched GDGTs in soil.
617 *Org. Geochem.* **41**, 1171-1175.
- 618 Peterse F., Prins M. A., Beets C. J., Troelstra S. R., Zheng H., Gu Z., Schouten S., and Sinninghe
619 Damsté J. S. (2011) Decoupled warming and monsoon precipitation in East Asia over the last
620 deglaciation. *Earth Planet. Sci. Lett.* **301**, 256-264.
- 621 Peterse F., Schouten S., van der Meer J., van der Meer M. T. J., and Sinninghe Damsté J. S.
622 (2009b) Distribution of branched tetraether membrane lipids in geothermally heated soils:
623 implications for the MBT/CBT temperature proxy. *Org. Geochem.* **40**, 201-205.
- 624 Pitcher A., Hopmans E. C., Schouten S., and Sinninghe Damsté J. S. (2009) Separation of core
625 and intact polar archaeal tetraether lipids using silica columns: Insights into living and fossil
626 biomass contributions. *Org. Geochem.* **40**, 12-19.

- 627 Rueda G., Rosell-Melé A., Escala M., Gyllencreutz R., and Backman J. (2009) Comparison of
628 instrumental and GDGT-based estimates of sea surface and air temperatures from the
629 Skagerrak. *Org. Geochem.* **40**, 287-291.
- 630 Schouten S., Eldrett J., Greenwood D. R., Harding I., Baas M., and Sinninghe Damsté J. S.
631 (2008) Onset of long-term cooling of Greenland near the Eocene-Oligocene boundary as
632 revealed by branched tetraether lipids. *Geology* **36**, 147-150.
- 633 Schouten S., Hugué C., Hopmans E. C., Kienhuis M. V. M., and Sinninghe Damsté J. S. (2007)
634 Analytical methodology for TEX86 paleothermometry by high-performance liquid
635 chromatography/atmospheric pressure chemical ionization-mass spectrometry. *Anal. Chem.*
636 **79**, 2940-2944.
- 637 Schouten S., Middelburg J. J., Hopmans E. C., and Sinninghe Damsté J. S. (2010) Fossilization
638 and degradation of intact polar lipids in deep subsurface sediments: A theoretical approach.
639 *Geochim. Cosmochim. Acta* **74**, 3806-3814.
- 640 Sinninghe Damsté J. S., Hopmans E. C., Pancost R. D., Schouten S., and Geenevasen J. A. J.
641 (2000) Newly discovered non-isoprenoid glycerol dialkyl glycerol tetraether lipids in
642 sediments. *Chem. Commun.* 1683-1684.
- 643 Strous M., Heijnen J. J., Kuenen J. G., and Jetten M. S. M. (1998) The sequencing batch reactor
644 as a powerful tool for the study of slowly growing anaerobic ammonium-oxidizing
645 microorganisms. *Appl. Microbiol. Biotechnol.* **50**, 589-596.
- 646 Van de Graaf A. A., de Bruijn P., Robertson L. A., Jetten M. S. M., and Kuenen J. G. (1996)
647 Autotrophic growth of anaerobic ammonium-oxidizing micro-organisms in a fluidized bed
648 reactor. *Microbiology-UK* **142**, 2187-2196.
- 649 Weijers J. W. H., Panoto E., Van Bleijswijk J., Schouten S., Rijpstra W. I. C., Balk M., Stams A.
650 J. M., and Sinninghe Damsté J. S. (2009) Constraints on the biological source(s) of the orphan
651 branched tetraether membrane lipids. *Geomicrobiol. J.* **26**, 402-414.
- 652 Weijers J. W. H., Schefuß E., Schouten S., and Sinninghe Damsté J. S. (2007a) Coupled thermal
653 and hydrological evolution of tropical Africa over the last deglaciation. *Science* **315**, 1701-
654 1704.
- 655 Weijers J. W. H., Schouten S., Hopmans E. C., Geenevasen J. A. J., David O. R. P., Coleman J.
656 M., Pancost R. D., and Sinninghe Damsté J. S. (2006a) Membrane lipids of mesophilic
657 anaerobic bacteria thriving in peats have typical archaeal traits. *Environ. Microbiol.* **8**, 648-
658 657.
- 659 Weijers J. W. H., Schouten S., Sluijs A., Brinkhuis H., and Sinninghe Damsté J. S. (2007b)
660 Warm Arctic continents during the Palaeocene-Eocene thermal maximum. *Earth Planet. Sci.*
661 *Lett.* **261**, 230-238.

- 662 Weijers J. W. H., Schouten S., Spaargaren O. C., and Sinninghe Damsté J. S. (2006b)
663 Occurrence and distribution of tetraether membrane lipids in soils: Implications for the use of
664 the TEX₈₆ proxy and the BIT index. *Org. Geochem.* **37**, 1680-1693.
- 665 Weijers J. W. H., Schouten S., van den Donker J. C., Hopmans E. C., and Sinninghe Damsté J. S.
666 (2007c) Environmental controls on bacterial tetraether membrane lipid distribution in soils.
667 *Geochim. Cosmochim. Acta* **71**, 703-713.
- 668 Weijers J. W. H., Wiesenberg G. L. B., Bol R., Hopmans E. C., and Pancost R. D. (2010) Carbon
669 isotopic composition of branched tetraether membrane lipids in soils suggest a rapid turnover
670 and a heterotrophic life style of their source organism(s). *Biogeosciences* **7**, 2959-2973.
671
672
673
674
675
676
677
678

679 **Figure captions**

680

681 Fig.1: Overview of reconstructed annual mean air temperatures using the MBT-CBT proxy
682 (triangles) and the measured annual mean air (grey horizontal bar) and soil (brown
683 horizontal bar) temperatures among the different soils. The range in monthly average air
684 temperatures is indicated by the grey surface area; the range in monthly average soil
685 temperature is indicated by the vertical brown bars. Note that the vertical bars behind the
686 triangles do not represent the standard error of the mean but represent the total range in
687 temperatures reconstructed with the MBT-CBT proxy during the year. Triangles are
688 color-coded: green represent core lipid (CL) branched GDGTs, red represents intact polar
689 lipid (IPL)-derived branched GDGTs upon acid (H) hydrolysis, and blue represents IPL-
690 derived branched GDGTs derived upon base (OH) hydrolysis, see also bottom axis.

691

692 Fig. 2: Concentrations of branched GDGTs over the one-year time series analyzed in the
693 different soils. A) core lipids (CLs) in the soils at Itasca State Park, Minnesota, USA; B)
694 CLs in the soils at Bath Nature Preserve, Ohio, USA; C) CLs and intact polar lipid (IPL)-
695 derived branched GDGTs in the grassland soil at Texel, The Netherlands; and D) CLs,
696 total IPL-derived branched GDGTs and branched GDGTs derived from phosphate-bound
697 IPLs in the grassland soil from Rowden Moor, UK.

698

699 Fig. 3: MBT-CBT reconstructed MATs (dots) for A) the open field soil; B) the pine forest soil;
700 and C) the deciduous forest soil at Itasca State Park, Minnesota, USA, plotted against the
701 daily mean air temperature (grey line) and daily mean soil temperature at 15 cm depth
702 (black line). The horizontal grey striped line represents the measured annual MAT and
703 the horizontal black striped line the measured annual mean soil temperature at the site.
704 Note that the soil temperature curve in graph C is actually the soil temperature measured
705 in the pine forest soil (see text).

706

707 Fig. 4: MBT-CBT reconstructed MATs (dots) for A) the open field soil; B) the pine forest soil;
708 and C) the deciduous forest soil at Bath Nature Preserve, Ohio, USA, plotted against the
709 daily mean air temperature (grey line) and daily mean soil temperature at 15 cm depth

710 (black line). The horizontal grey striped line represents the measured annual MAT and
711 the horizontal black striped line the measured annual mean soil temperature at the site.
712 Note that the soil temperature curve in graph C is actually the soil temperature measured
713 in the pine forest soil (see text).

714

715 Fig. 5: MBT-CBT reconstructed MATs based on core lipid (CL, black circles) and intact polar
716 lipid (IPL, white squares)-derived branched GDGTs, for the grassland soil at Texel, The
717 Netherlands, plotted against monthly mean air temperature (black line) and the measured
718 soil temperature at 10 cm depth at the time of sampling (black crosses).

719

720 Fig. 6: MBT-CBT reconstructed MATs based on branched GDGT core lipids (CL, black
721 circles), IPL-derived branched GDGTs after acid hydrolysis (white squares) and IPL-
722 derived branched GDGTs after base hydrolysis (white diamonds), for the grassland soil at
723 Rowden Moor, UK, plotted against measured daily mean air temperature (grey line) and
724 measured daily mean soil temperature at 10 cm depth (black line).

725

726

727

Figure 1

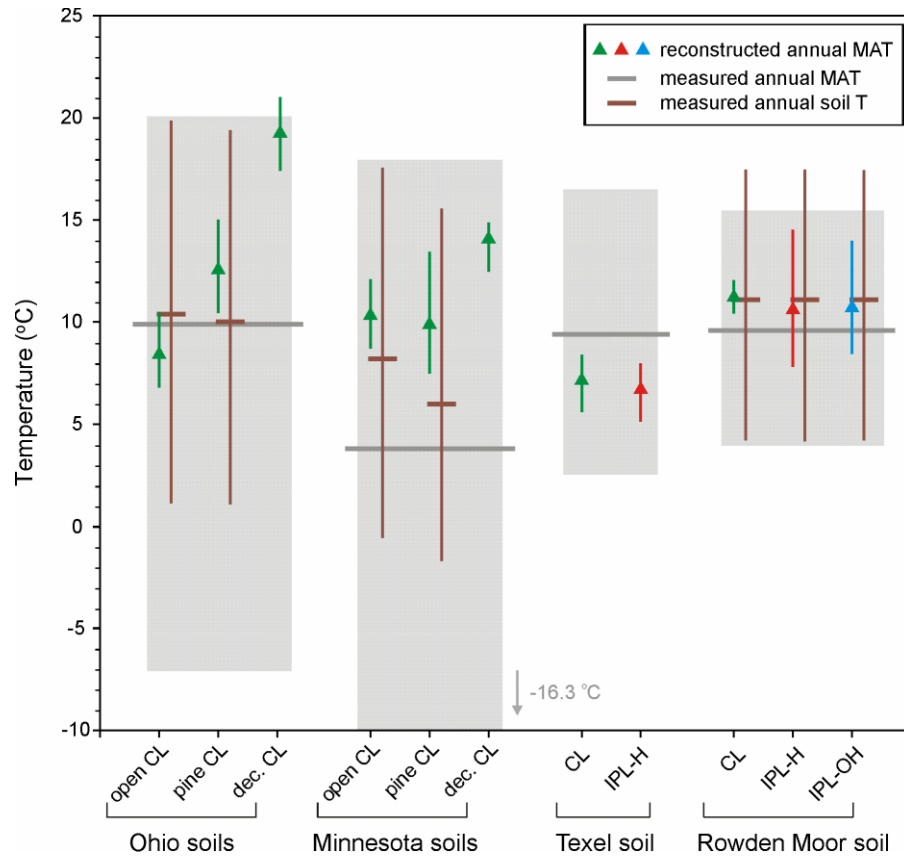


Figure 2

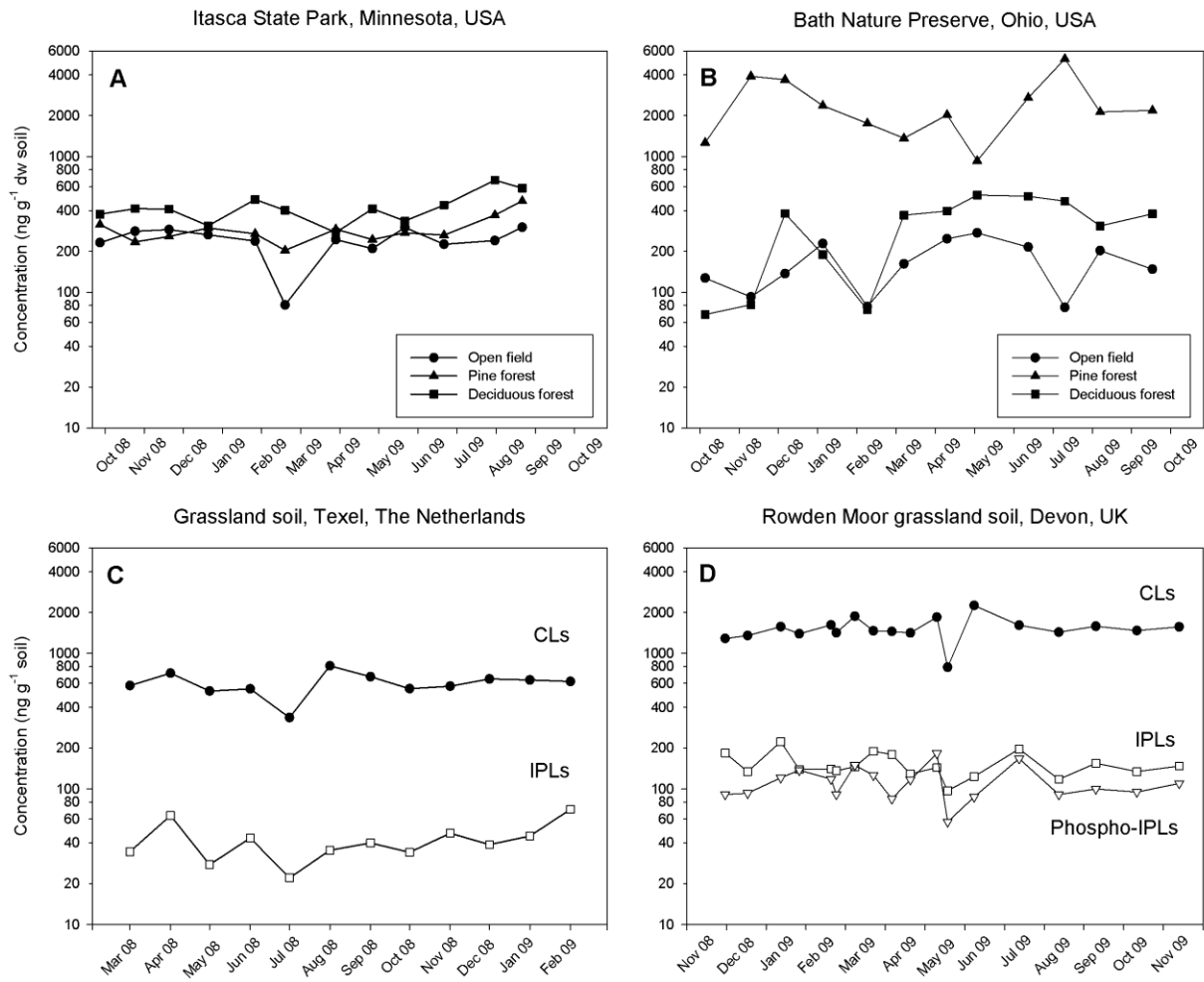


Figure 3

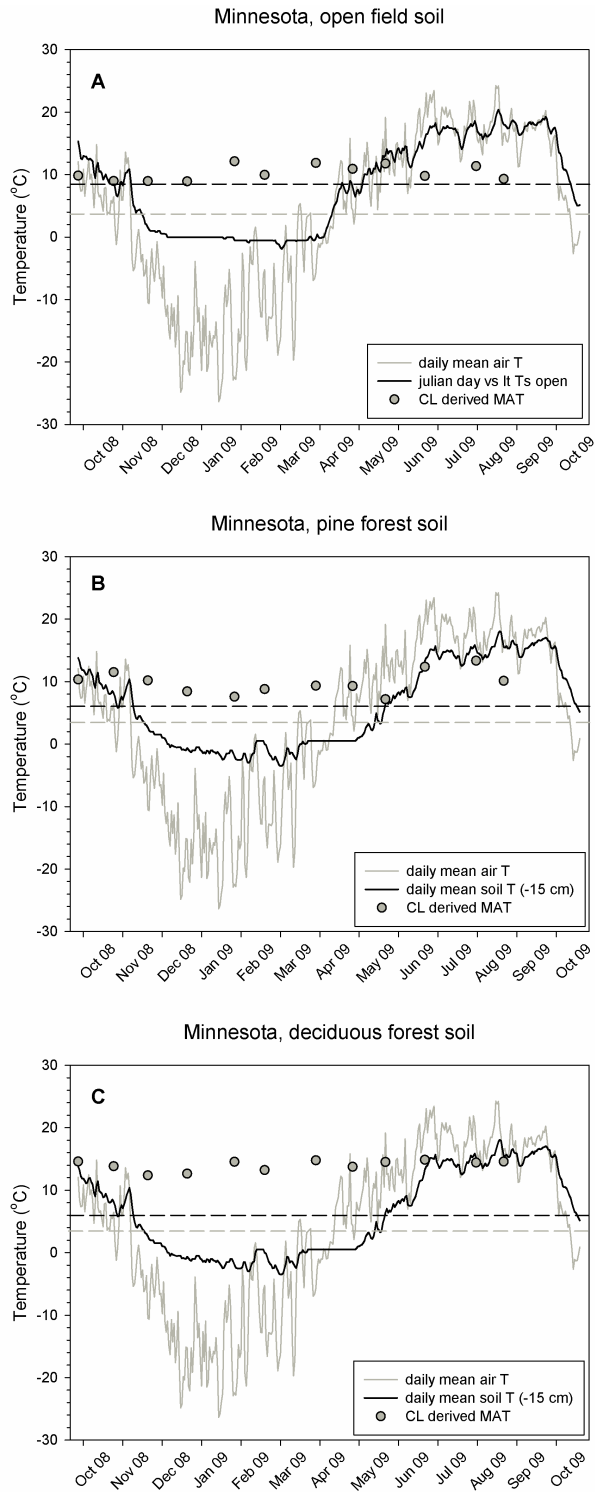


Figure 4

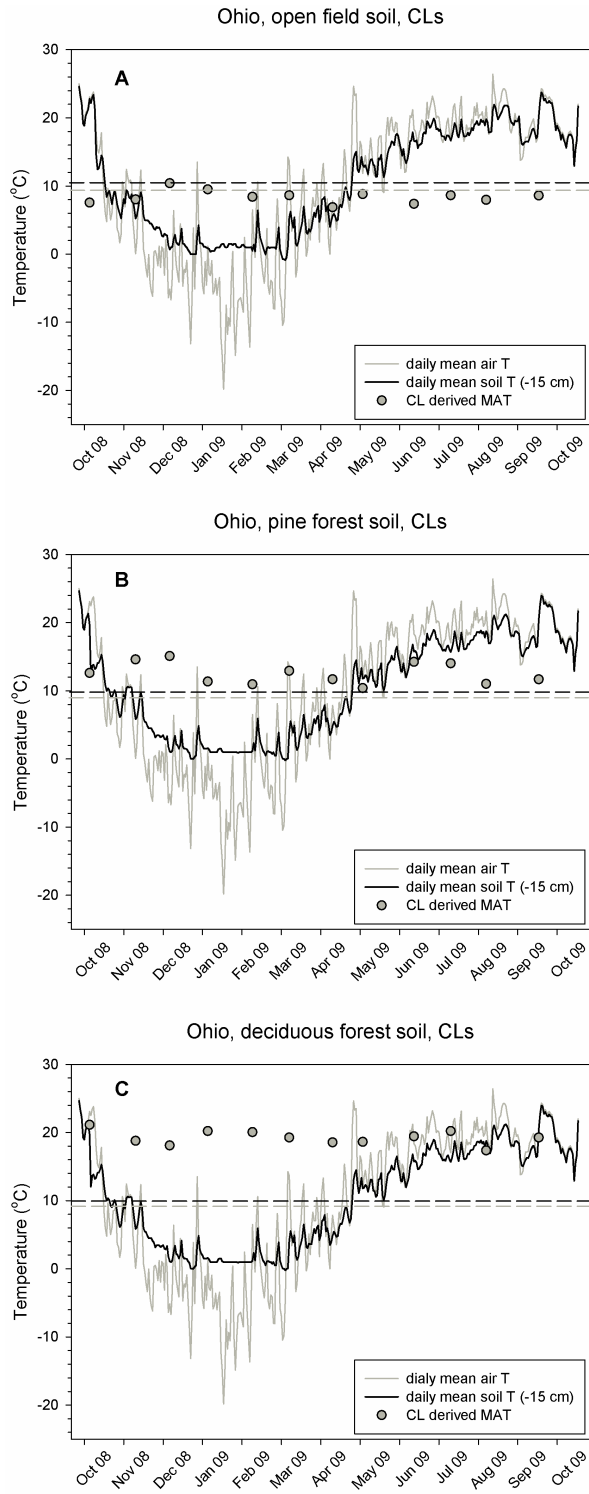


Figure 5

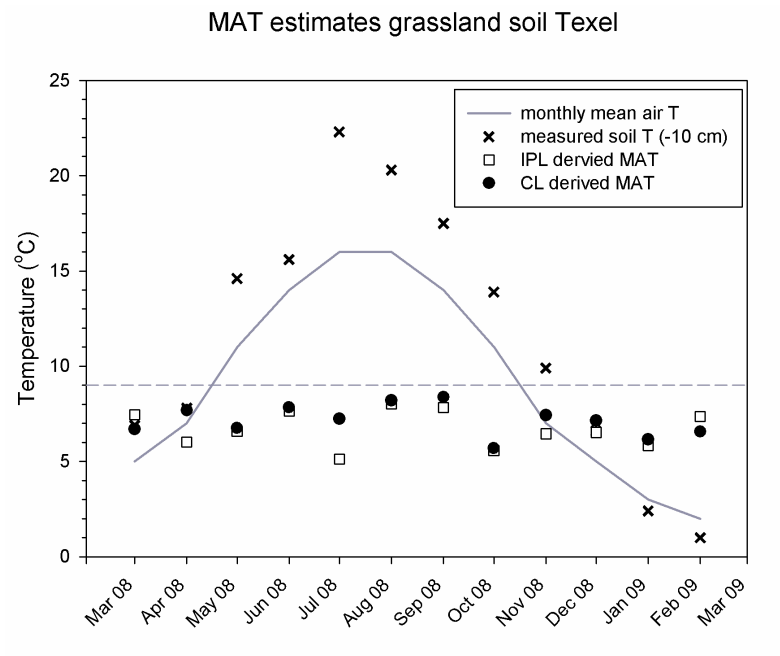


Figure 6

